V-Grooved Substrate Buried Heterostructure InGaAsP/InP Laser Emitting at 1.3 μm Wavelength

HIROSHI ISHIKAWA, HAJIME IMAI, MEMBER, IEEE, TOSHIYUKI TANAHASHI, KEN-ICHI HORI, AND KENICHIRO TAKAHEI

Abstract—**Details of the fabrication, optimization of the dimensions of the active region, characteristics, and the aging results of the V-grooved substrate buried heterostructure (VSB) InGaAsP/InP laser are described. It is shown that the VSB laser can be fabricated in one-step epitaxy as well as two-step epitaxy. The active region width below 2.5 μm and the thickness of 0.15-0.2 μm are shown to give stable fundamental mode operation and good temperature characteristics. The fundamental mode operation up to the optical output of 20 mW/facet at 25°C and the CW operation above 100°C are obtained. The pulse response showed the strongly damped relaxation oscillation with a frequency as high as 4.5 GHz. The spectral width under the modulation of 400 Mbit/s RZ single is as narrow as 25 Å in full width at half maximum. Highly stable aging characteristics at an elevated temperature of 50°C are obtained in both two-step epitaxy lasers and one-step epitaxy lasers.**

I. INTRODUCTION

THE need for practical lasers for high bit rate optical communication systems at a wavelength of 1.3 and 1.5 μm increased largely due to the development of the very low loss and small dispersion optical fiber at these wavelength regions [1]. To this end various types of the stripe geometry InGaAsP/InP lasers have been developed [2]-[11]. Among them BH type lasers are promising due to their very low threshold current. The low threshold current laser enables us to operate the laser at high ambient temperature due to its small power dissipation. This is especially important in quaternary lasers because of the small T_0 value. Further, the low threshold current laser realizes a high bit rate modulation because the laser can be operated at a high ratio of the driving current to the threshold current which leads to the high relaxation oscillation frequency. Very low threshold current BH lasers [3], [4] and buried crescent laser [5] have been reported. However, the BH type lasers hitherto reported are rather complicated in their structure. We have recently reported a new simple structure laser, namely the V-grooved substrate buried heterostructure (VSB) laser emitting at 1.3 μm wavelength [12]. The VSB laser showed a very low threshold current of 10–20 mA, smooth far field pattern, and strongly damped relaxation oscillation with high frequency. Owing to its simple structure, we have recently developed a one-step epitaxy VSB laser using a diffusion process for the formation of the internal current restriction layer [13].

Manuscript received March 9, 1982.

H. Ishikawa, H. Imai, T. Tanahashi, and K.-I. Hori are with Fujitsu Laboratories, Ltd., Kawasaki, Japan.

K. Takahei is with the Musashino Electrical Communications Laboratory, Nippon Telegraph and Telephone Public Corporation, Tokyo, Japan.

In this paper we report the details of the fabrication process, the optimization of the width and the thickness of the active region, characteristics, and aging results at elevated temperature. In the description of the fabrication process, we show the etching property of (100) InP, the fabrication of the two-step epitaxy VSB laser, and the fabrication of one-step epitaxy VSB laser. The realization of the one-step epitaxy laser shows the possibility of obtaining low cost lasers. The optimization of the dimensions of the active region is carried out experimentally to yield the stable fundamental mode operation and the good temperature characteristics. The fundamental mode operation up to the optical output of 20 mW/facet at 25°C, and CW operation up to 100°C are realized. The longitudinal mode characteristics and the modulation characteristics are also examined. It is shown that the VSB laser is suited for high bit rate optical communication systems. The aging test at elevated temperature is performed mainly for two-step epitaxy lasers. We have obtained the most stable aging result so far reported in quaternary lasers. The preliminary aging test for the one-step epitaxy laser is also performed and a stable aging result comparable to that of the two-step epitaxy laser is obtained.

II. STRUCTURE AND FABRICATION

A. Structure

The schematic cross section of the VSB laser and the scanning electron microscope photograph of it are shown in Fig. 1(a) and (b), respectively. The crescent-shaped active region is buried in the V-shaped groove whose facet is exactly (111)*B* facet. The current restriction to the active region is realized by the p-n-p-n layer structure outside of the stripe which consists of p-InGaAsP cap layer (layer 5), p-InP clad layer (layer 4), very thin InGaAsP undoped layer (layer 3), n-InP clad layer (layer 2), p-InP current restriction layer (layer 1), and the substrate. The VSB laser has the following advantages in its structure.

1) The structure is simple and it can be fabricated even in one-step epitaxy using the diffusion process for the formation of the internal current restriction layer (layer 1).

2) A far field pattern without irregularity is obtained, owing to the alignment of the active region edge to the highly smooth facet of the V-groove.

3) We can obtain a flat surface of the wafer, then the stress, when bonded p-side down is small.

4) As the active layer is not exposed to high ambient temperature in the regrowth process, we can expect long lived lasers.

0018-9480/82/1000-1692$00.75

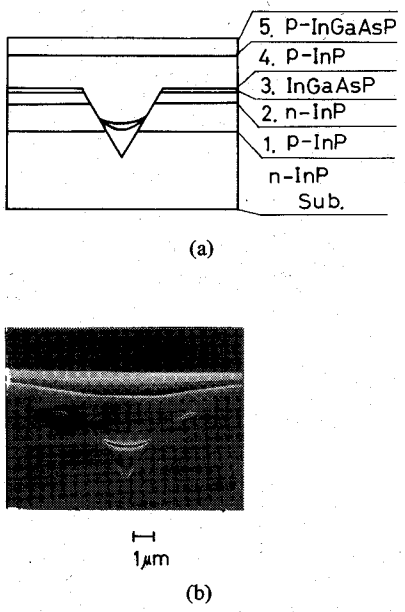

Fig. 1. The schematic cross section and the scanning electron microscope photograph of the VSB laser.

Prior to deciding the structure of the VSB laser with the above advantages, we have examined the etching property of InP to select the groove for the new structure laser.

B. Etching Property (100) InP

The etching property of the (100) surface of InP was examined using three types of etchants; $HCl:HNO_3$, $HCl:H_3PO_4$, and $Br_2:CH_3OH$. Also discussed by Adachi *et al.* [14], InP has an interesting etching property. Fig. 2 shows various types of grooves formed by the above three etchants. When the direction of the stripe is $\langle 01\bar{1} \rangle$, we obtain two types of the groove: those that are *V*-shaped as shown in Fig. 2(d) and (e). The facet of the *V*-groove [Fig. 2(d)] is (111)*A* surface, and that of the groove [Fig. 2(e)] is (211). In these two grooves, we find that reproducible liquid phase epitaxial growth is very difficult. This is consistent with the report for the groove [Fig. 2(d)] by Murotani *et al.* [5]. When the stripe direction is $\langle 011 \rangle$, we obtain three types of grooves: (a), (b), and (c). Contrary to the grooves in the $\langle 01\bar{1} \rangle$ direction, growth can easily be performed in these grooves. However, groove (c) is not appropriate for our purpose because the width of the active region becomes wider than the mask width when the active region is buried in this groove. Further, the melt-etching of the corner of the groove is liable to take place. Fig. 3 shows the scanning electron microscope photograph of the groove (a) and (b). A highly smooth surface of the *V*-groove (a) is obtained. The surface is identified to be exactly (111)*B* facet. Although the groove (b) can be formed with small side etching, the groove with small width can be realized; the side wall of the groove (b) is not a specific surface of the crystal and is irregular. As the irregularity in the far field pattern of the BH type laser is considered to be due to the irregular active region edge [2], [15], we do not take the groove (b) for the new structure laser. Thus, the groove (a) with (111)*B* facet is selected for the new structure BH type laser. However, it is

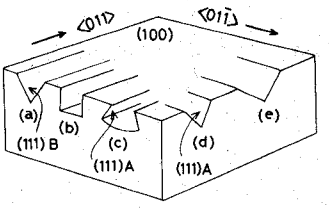

(a) $HCl-H_3PO_4$ (HCl rich)
(b) $HCl-HNO_3$
(c),(d) Br_2-CH_3OH
(e) $HCl-H_3PO_4$, $HCl-HNO_3$

Fig. 2. Various grooves formed on (100) InP by chemical etching.

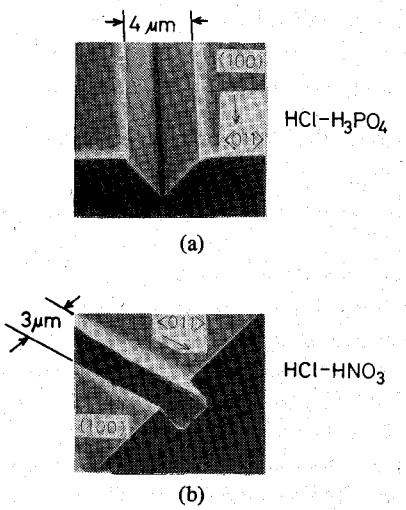

Fig. 3. Scanning electron microscope photograph of the groove (a) and groove (b) in Fig. 2.

worth mentioning that the very low threshold current laser comparable to the VSB laser can be fabricated using the groove (b) [15].

C. Fabrication of Two-Step Epitaxy Laser

In the fabrication, the Sn doped substrate with carrier concentration of $2 \times 10^{18}/cm^3$ was used. At first, the p-InP layer with a thickness of 1.5 μm (Cd doped, $5 \times 10^{17}/cm^3$) is grown on (100) surface of the substrate. Then a SiO_2 mask is deposited and the groove (a) is formed. The typical width of the groove is 3.5–4 μm. After the formation of the groove, an n-InP clad layer (Sn doped, $5 \times 10^{17}/cm^3$), undoped active layer of 1.3 μm wavelength, p-InP clad layer (Cd doped, 5×10^{17}), and InGaAsP cap layer (Zn doped, $1 \times 10^{19}/cm^3$) are grown successively. The growth temperature is 600°C. The merit of the VSB laser in the fabrication is that the width of the active region can be controlled by the position of the active region in the *V*-shaped groove owing to the fixed angle of *V*. We obtain a width narrower than 2.5 μm by setting the active region below the position of 1.5 μm from the bottom of the *V*.

After the epitaxial growth, p- and n-contacts are formed. For the p-type contact, Ti-Pt-Au is used and for the n-type contact AuGeNi is used. Samples are bonded p-side down on a diamond heat sink using AuSn alloy bonding solder [16].

D. Fabrication of One-Step Epitaxy Laser

For the low cost fabrication of lasers, the one-step epitaxy is, of course, desirable. The one-step epitaxy laser can be fabricated using Cd diffusion for the formation of p-InP internal current restriction layer (layer 1). In the fabrication, the same substrate is used as that used for the two-step epitaxy layer. The diffusion of Cd is carried out in the closed tube system at the temperature of 600°C using CdP_2 as a source. The diffusion time is typically 3 h. The junction depth depends largely on P pressure. When red phosphor is introduced in the tube to apply the excess P pressure, the junction depth of 2.2 μm is obtained. While the depth is as deep as 3.5 μm when no red phosphor is introduced. We applied the excess P pressure to avoid heat damage of the substrate. After the diffusion, the surface of the as diffused wafer is etched by 0.5 μm to eliminate the high concentration layer near the surface. Then the same process as that of the two-step epitaxy laser follows.

E. Comparison of One-Step Epitaxy Laser and Two-Step Epitaxy Laser

Fig. 4 shows the V-I characteristics of the VSB laser diode and that of the p-n-p-n structure outside of the stripe. The size of the p-n-p-n structure measured is 250 X 200 μm^2. Two cases are shown for the p-n-p-n structure; structure by LPE alone and that by one-step epitaxy with diffusion process. The current of the p-n-p-n structure for the forward bias voltage of 4 V is less than 500 μA. We can see that the p-n-p-n structure, enough for the current restriction, is realized both in two-step epitaxy and in one-step epitaxy with diffusion process. This is also true at elevated temperature as evidenced in the V-I characteristics at 70°C in Fig. 4.

Fig. 5 shows the pulsed I-L characteristics of two kinds of samples. Samples are side by side in one wafer. The width of the active region is 2.2 μm and the thickness measured at the center is 0.17 μm in both wafers. We can see that the very low threshold current typically of 12 mA is reproducibly obtained in both wafers.

In the following, we report the characteristics mainly obtained in two-step epitaxy lasers. This is simply because the two-step epitaxy laser is initially developed and we have enough data for the two-step epitaxy lasers. However, the results obtained hereafter will equally apply to the one-step epitaxy laser with diffusion process because we have found no obvious difference in the characteristics so far [13].

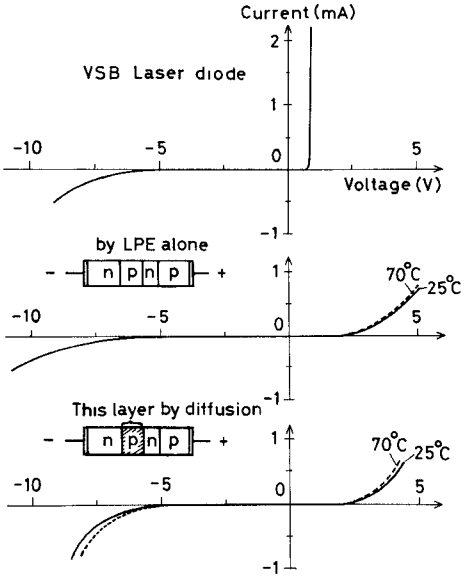

Fig. 4. V-I characteristics of the VSB laser diode and that of p-n-p-n structure outside of this stripe. Two cases are shown for the p-n-p-n structure: structure by two-step epitaxy (LPE alone) and that by one-step epitaxy with diffusion process.

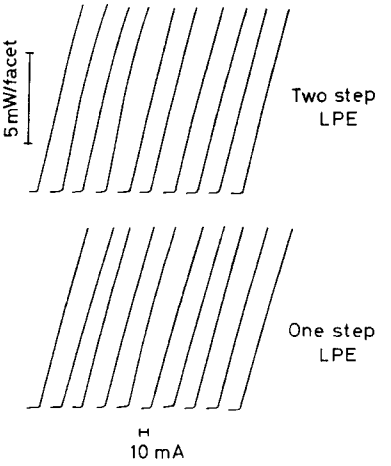

Fig. 5. Pulsed I-L characteristics of the samples. Samples are side by side in one wafer. Two cases are shown: samples from two-step epitaxy wafer and those from one-step epitaxy wafer.

III. Optimization of the Active Region Dimensions

A. Outline of the Optimization

The thickness and width of the active region should be determined such that the stable fundamental mode lasing, low threshold current, high differential quantum efficiency, and good temperature characteristics are obtained. However, the theoretical optimization is very difficult because of the crescent-shaped active region which makes it very difficult to calculate the optical field exactly. The calculation of the optical field using the effective refractive index approximation was reported by Kirkby *et al.* for GaAlAs channeled substrate buried heterostructure laser with a crescent-shaped active region [17] and similar calculation was applied to the buried crescent stripe geometry InGaAsP/InP laser by Oomura *et al.* [18]. A useful result such as the cutoff condition of the higher order modes was obtained. However, the analysis remains approximate and, above all, the evaluation of the optical confinement factor in the vertical direction taking account of the lateral thickness variation is not performed. For the analysis of the dependence of the threshold current and the differential quantum efficiency on the active region thickness, the calculation of the optical confinement factor in a vertical direction is inevitable. Under such conditions, we have taken the experimental procedure for the optimization of the active region dimensions.

Lasers with various active region thicknesses and widths were fabricated and the relation between the characteristics and the cross-sectional dimensions of each laser was examined. We obtained the dependence of the threshold current density, differential quantum efficiency, and the temperature charac-

teristics on the active region thickness. The relation between the lasing transverse mode, fundamental or higher order mode, and the dimensions of the active region was examined.

B. Threshold Current Density, Differential Quantum Efficiency, and Temperature Characteristics

Fig. 6 shows the dependence of the threshold current density and the differential quantum efficiency in CW at 25°C on the active region thickness d_0, which is measured at the center of the crescent-shaped active region. The differential quantum efficiency is defined as a slope between the 5 mW/facet output and the threshold. We can see that the dependence of the threshold current density on the active region thickness d_0 is slight, while the differential quantum efficiency increases when the active region thickness is reduced. The threshold current density is typically 2.5-3 kA/cm^2, and the differential quantum efficiency increases from 35 to 50 percent when the thickness is reduced. These results can be qualitatively understood as follows. The thickness d_0 in the range of 0.05-0.2 μm corresponds to the minimum of the threshold current density and, in this thickness region, the dependence of the threshold current density on d_0 is similar to the laser with a flat active layer. While in this thickness region the optical confinement factor in the vertical direction decreases rapidly as the thickness is reduced, as can be estimated from the analysis for a flat active layer laser [19]. The reduction of the optical confinement factor reduces the free carrier absorption in the active layer and hence, results in the increase in the differential quantum efficiency.

Fig. 7 shows the dependence of the temperature characteristics on the thickness d_0. The ratio of the CW threshold current at 50°C to that at 25°C is plotted. On the right-hand side coordinate, the corresponding T_0 value is shown. We can see that the temperature characteristics deteriorate as the thickness is reduced. To obtain a T_0 value larger than 45 K, it is required to make the thickness d_0 above 0.15 μm. The cause of the deterioration of the temperature characteristics when the thickness is reduced could be the carrier leakage across the heterobarrier [20]-[22], which is enhanced by the long energy relaxation time of electrons in the conduction band [23], giving a higher electron temperature than the lattice temperature [24]. Such deterioration of the temperature characteristics would appear prominently in the lasers with a crescent-shaped active region because the active region has very thin portions on both sides.

C. Fundamental Transverse Mode Lasing Condition

Fig. 8 shows the dependence of the lasing transverse mode in a lateral direction, fundamental or higher order, on the width and thickness of the active region. The plot by ○ is the sample that lased in fundamental transverse mode, by × is the sample lased in first order, and by □ is the sample lased in second order. In the experiment, the far field pattern is measured up to the optical output power of 5 mW/facet. Samples that showed the broadening of the far field pattern when the injection current is increased is counted as a sample in higher order mode because the broadening of the far field pattern is the indication of the changing into higher order mode. For comparison, we have shown the calculated first order mode cutoff condition by Oomura *et al.* [18]. From Fig. 8, we can see that the fundamental mode lasing above 5 mW/facet can be obtained even when the first order mode cutoff condition is not strictly satisfied. This would be due to the difference in the optical loss between the fundamental and first order mode. We find a similar situation in the buried convex waveguide stripe laser at 0.8 μm wavelength [25].

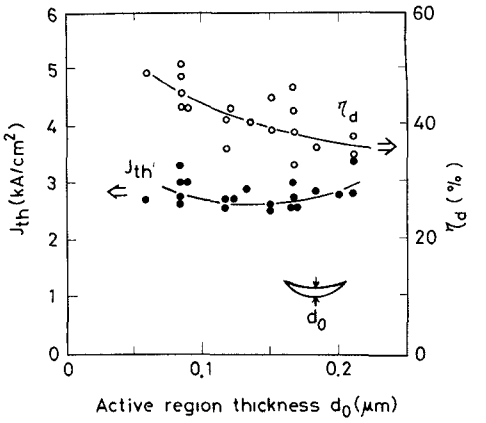

Fig. 6. Dependence of the CW threshold current density and the differential quantum efficiency on the thickness d_0 of the active region.

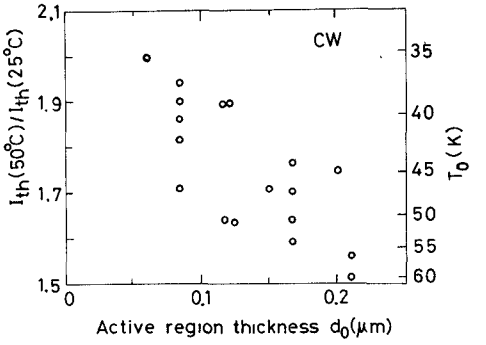

Fig. 7. Dependence of the temperature characteristics on the active region thickness d_0. The temperature characteristics deteriorate when d_0 is reduced.

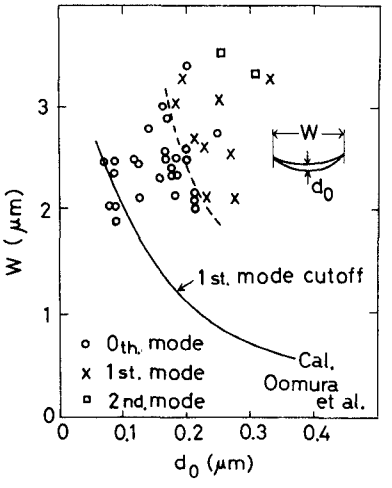

Fig. 8. Relation between the lasing mode, fundamental or higher order, on the width and the thickness of the active region.

D. Characteristics of Optimized Laser

From the results of A, B, and C the thickness of the active region d_0 in the range 0.15-0.20 μm and the width below the dashed line in Fig. 8 would be optimum to obtain a stable fundamental transverse mode lasing above 5 mW/facet output and good temperature characteristics. We obtain the T_0 value of 45-55 K in this thickness region and differential quantum efficiency of 35-45 percent as can be read from Figs. 6 and 7.

Fig. 9 shows the I-L characteristics and the corresponding far field pattern of the optimized laser, i.e., the width of the active region is 2.5 μm and the thickness is 0.17 μm. A stable fundamental mode operation up to the optical output power of 20 mW/facet is obtained. Fig. 10 shows the far field pattern in the vertical direction. Full width at half maximum (FWHM) is 32°. The FWHM in the vertical direction for the active region thickness of 0.15-0.2 μm was typically in the range 30-40° and that in the horizontal direction was 23-30° for the active region width of 2.0-2.5 μm.

It should be noticed in Fig. 9 that the far field pattern is smooth when compared with the conventional BH type laser [3]. This is owing to the fact that the active layer edge aligns to the smooth facet of the V-groove.

Fig. 11 shows the temperature dependence of the CW I-L characteristics. Through the optimization, the CW lasing up to 100°C is realized. The ratio of the CW threshold current at 50°C to that at 25°C is 1.6, which corresponds to the T_0 value of 55 K.

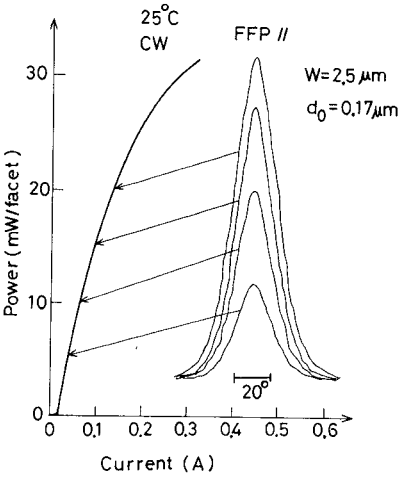

Fig. 9. I-L characteristics and the corresponding far field pattern lateral to the stripe direction of the optimized VSB laser.

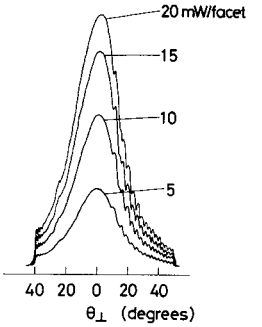

Fig. 10. Far field pattern perpendicular to the junction plane of the sample shown in Fig. 9.

IV. Longitudinal Mode and Dynamic Characteristics

A. Longitudinal Mode Characteristics Under CW Operation

Fig. 12 shows the typical lasing spectrum when the dc injection current is changed. The VSB laser has a tendency to lase in multiple longitudinal modes, in contrast to the separated multiclad layer stripe geometry laser which shows a highly pure single longitudinal mode lasing [26]. The multiple tendency of the VSB laser would be due to the spatial inhomogeneity of the active region that still remains in the longitudinal direction, and also due to the fact that the crescent-shaped waveguide is not under the condition of the first order mode cutoff. Recently, Yamada *et al.* showed that the existence of the higher order transverse mode prevents the gain suppression around the lasing mode [27]. Although the VSB laser lases in multiple longitudinal modes, the FWHM of the envelope of the spectrum is typically below 30 Å. An improvement could be done by increasing the spatial homogeneity and by making the first order mode under cutoff.

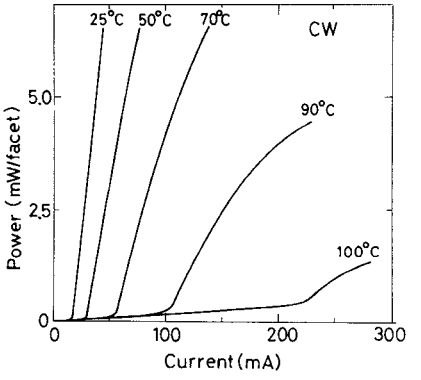

Fig. 11. Temperature dependence of the CW I-L characteristics.

B. Dynamic Characteristics

For high bit rate modulation of the laser diode, the relaxation oscillation frequency must be several times higher than that of the modulation bit rate. The relaxation oscillation frequency f_r is approximately given by [28]

$$f_r = \frac{1}{2\pi}\frac{1}{\sqrt{\tau_p \tau_s}}((I_b + I_d)/I_{\text{th}} - 1)^{1/2} \quad (1)$$

where τ_s is the spontaneous carrier lifetime, τ_p is the photon lifetime, I_b is the bias current, and I_d is the high frequency modulation current. We can readily see that high relaxation oscillation frequency can be realized by making the ratio $(I_b + I_d)/I_{\text{th}}$ large. This is attained in the VSB laser because of its very low threshold current.

Fig. 13 shows the pulse response for various pulse amplitudes. The bias current is set at threshold. We can see that relaxation oscillation is strongly damped. Fig. 14 shows the relaxation oscillation frequency as a function of the overdrive $(I_b + I_d)/I_{\text{th}} - 1$ for three samples. We obtain the slope of $\frac{1}{2}$ indicating

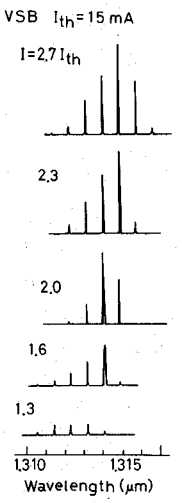

Fig. 12. Typical lasing spectrum under CW operation for various injection current levels.

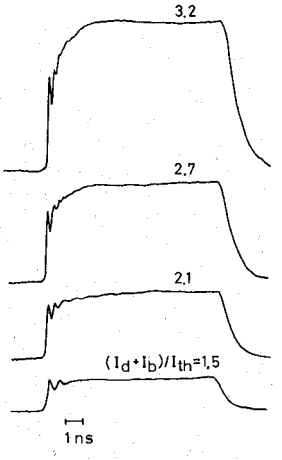

Fig. 13. Pulse response for various injection current levels. The bias current is set at threshold.

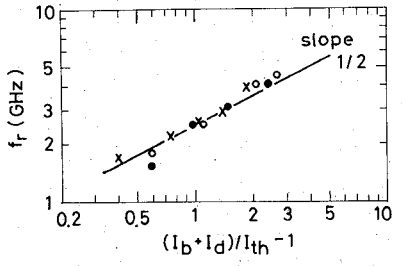

Fig. 14. Relaxation oscillation frequency as a function of the overdrive $(I_b + I_d)/I_{th} - 1$. A slope of $\frac{1}{2}$ is obtained.

that the relaxation oscillation frequency is well expressed by (1). A frequency as high as 4.5 GHz is obtained. From Fig. 14 we obtain $\tau_p \tau_s$ of 4.05×10^{-21} s^2.

Fig. 15 shows the modulation waveform under 400 Mbit/s RZ random pulse current. The bias current is set at 0.8 times the threshold current and the pulse amplitude is adjusted so that the peak optical output power is 5 mW/facet. Fairly good eye pattern is obtained. Fig. 16 shows the example of the spectrum under 400 Mbit/s RZ random pulse modulation. The spectrum is almost the same as that under CW operation

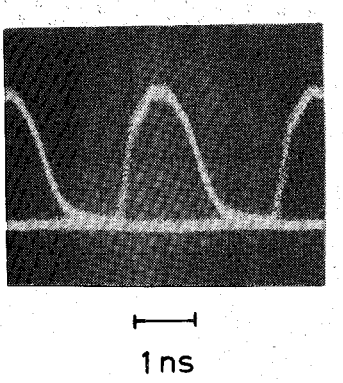

Fig. 15. Modulation waveform for 400 Mbit/s RZ random pulse current. The bias current is 0.8 times the threshold current and the pulse amplitude is adjusted so that the peak optical output power is 5 mW/facet.

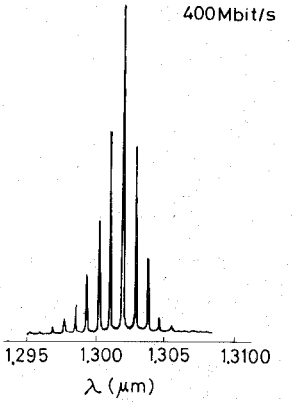

Fig. 16. Spectrum under the modulation of 400 Mbit/s RZ random pulse current.

and the FWHM of the envelope of the spectrum is 25 Å. This spectral width under modulation is enough for the 400 Mbit/s optical transmission system at 1.3 μm wavelength.

V. Aging Characteristics

The aging test is performed at an elevated temperature of 50°C with constant optical output power of 5 mW/facet. Fig. 17 shows the change in the driving current of the two-step epitaxy lasers. The driving current is in the range 60–80 mA. 15 samples are operated over 5000 h. We have observed no appreciable increase in the driving current so far. The average increase rate of the driving current is less than 1×10^{-6}/h, which is below the measurement error. Fig. 18 shows the preliminary aging result of the one-step epitaxy lasers. Four samples are operated over 3000 h. We can see that the one-step epitaxy lasers by the diffusion process also show the stable aging result comparable to that of the two-step epitaxy lasers.

We have reported a stable aging result of self-aligned structure laser, which showed the average increase rate of the driving current of 4.8×10^{-6}/h at the operation condition of 5 mW/facet at 50°C [29]. That was the most stable aging result so far reported in quaternary lasers. But the result obtained here in the VSB laser is the best data so far reported. One of the possible causes of the result would be the structure of the VSB

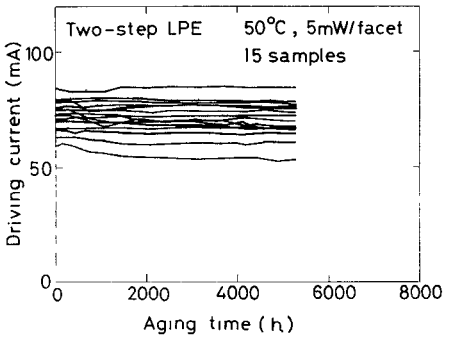

Fig. 17. The change in the driving current when samples are operated at 50°C, 5 mW/facet constant optical output power. Samples are two-step epitaxy laser.

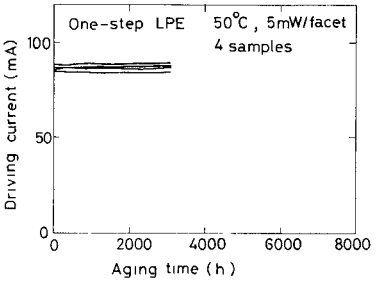

Fig. 18. The change in the driving current when samples are operated at 50°C, 5 mW/facet constant optical output power. Samples are one-step epitaxy lasers with diffusion process.

laser, i.e., the active region is not exposed to high ambient temperature in the regrowth process. It is interesting to note that the highly compensated p-InP layer in the one-step epitaxy laser does not seem to affect the reliability.

VI. Summary

A new simple structure VSB laser is developed. For the development of the VSB laser, the etching property of (100) InP was examined. It was shown that the V-shaped groove with (111)B facet can be formed. Using the groove, the VSB laser was developed in two-step epitaxy at first. It was also confirmed that the VSB laser can be fabricated in one-step epitaxy.

The width and the thickness of the active region were optimized experimentally. Stable fundamental mode lasing up to the optical output of 20 mW/facet at 25°C and CW operation up to 100°C were realized. The lasing spectrum of the VSB laser showed the multiple longitudinal mode lasing. However, the FWHM of the envelope was typically below 30 Å. The dynamic characteristics showed the strongly damped relaxation oscillation with a frequency as high as 4.5 GHz. The modulation waveform under 400 Mbit/s RZ random pulse current showed the well-opened eye pattern and the spectrum under modulation was as narrow as 25 Å in FWHM of the envelope. It is confirmed that the VSB laser is suited for the high bit rate optical communication systems.

The aging result of two-step epitaxy lasers at 50°C showed the most stable characteristics so far reported. The preliminary aging result of the one-step epitaxy laser also showed a similar result. We have obtained the reliable two-step epitaxy VSB lasers suited for the high bit rate optical communication systems, and confirmed the possibility of obtaining lasers in low cost by one-step epitaxy fabrication process.

Acknowledgment

The authors wish to thank T. Ikegami of Musashino Electrical Communication Laboratory, NTT, for his encouragement and discussions. They also wish to thank T. Misugi, K. Dazai, Y. Toyama, M. Takusagawa, and K. Akita for their incessant encouragement and advice. They are indebted to I. Umebu, Y. Nishiatani, I. Ushijima, S. Nakai, H. Sudo, and T. Kumai for their cooperation in the development of the VSB laser. They also wish to thank M. Motegi for the measurement of 400 Mbit/s modulation characteristics.

References

[1] T. Miya, Y. Terunuma, T. Hosaka, and T. Miyashita, "Ultimate low-loss single mode fiber at 1.55 μm," *Electron. Lett.*, vol. 15, pp. 106–108, Feb. 1979.

[2] J. J. Hsieh and C. C. Shen, "Room temperature CW operation of buried-stripe double-heterostructure GaInAsP/InP diode laser," *Appl. Phys. Lett.*, vol. 30, pp. 429–431, Apr. 1977.

[3] M. Hirao, S. Tsuji, K. Mizuishi, A. Doi, and M. Nakamura, "Long wavelength InGaAsP/Inp lasers for optical communication system," *J. Opt. Commun.*, vol. 1, pp. 10–14, Jan. 1980.

[4] H. Nagai, Y. Noguchi, K. Takahei, Y. Toyoshima, and G. Iwane, "InP/GaInAsP buried heterostructure lasers of 1.5 μm region," *Japan. J. Appl. Phys.*, vol. 19, pp. L218–L220, Apr. 1980.

[5] T. Murotani, E. Oomura, H. Higuchi, H. Namizaki, and W. Susaki, "InGaAsP/InP buried crescent laser emitting at 1.3 μm with very low threshold current," *Electron. Lett.*, vol. 16, pp. 566–567, July 1980.

[6] M. Yano, H. Nishi, and M. Takusagawa, "Oscillation characteristics in InGaAsP/InP DH lasers with self-aligned structure," *IEEE J. Quantum Electron.*, vol. QE-15, pp. 1388–1395, Dec. 1979.

[7] H. Ishikawa, H. Imai, K. Hori, Y. Nishitani, and M. Takusagawa, "Separated multi-clad layer stripe geometry InGaAsP/InP DH laser," presented at the 7th IEEE Semiconductor Laser Conf., Brighton, England, 1980, paper p31.

[8] H. Imai, H. Ishikawa, T. Tanahashi, and M. Takusagawa, "InGaAsP/InP separated multiclad layer stripe geometry laser emitting at 1.5 μm," *Electron. Lett.*, vol. 17, Jan. 1981.

[9] K. Kishino, Y. Suematsu, and Y. Itaya, "Fabrication and lasing property of mesa substrate buried heterostructure GaInAsP/InP lasers at 1.3 μm wavelength," *IEEE J. Quantum Electron.*, vol. QE-16, pp. 160–164, Feb. 1980.

[10] K. Wakao, K. Moriki, M. Kitamura, K. Iga, and Y. Suematsu, "$Ga_{1-x}Al_xAs_yP_{1-y}$/InP terraced substrate single-mode laser," *IEEE J. Quantum Electron.*, vol. QE-17, pp. 1009–1013, June 1981.

[11] W. J. Devlin, R. H. Walling, P. J. Fiddyment, R. E. Hobbs, D. Murrel, R. E. Spillett, and A. G. Steventon, "Low threshold current channeled-substrate buried crescent InGaAsP lasers emitting at 1.54 μm," *Electron. Lett.*, vol. 17, pp. 651–653, July 1981.

[12] H. Ishikawa, H. Imai, T. Tanahashi, Y. Nishitani, M. Takusagawa, and K. Takahei, "V-grooved substrate buried heterostructure InGaAsP/InP laser," *Electron. Lett.*, vol. 17, pp. 415–467, June 1981.

[13] H. Ishikawa, H. Imai, I. Umebu, K. Hori, and M. Takusagawa, "V-grooved substrate buried heterostructure InGaAsP/InP laser by one-step epitaxy," *J. Appl. Phys.*, Apr. 1982.

[14] S. Adachi and H. Kawaguchi, "Chemical etching characteristics of (100) InP," *J. Electrochem. Soc. Solid-State Science and Tech.*, vol. 128, pp. 1342–1349, June 1981.

[15] H. Ishikawa, H. Imai, T. Tanahashi, M. Takusagawa, and K. Takahei, "V-grooved substrate buried heterostructure InGaAsP/InP laser with smooth far field pattern and stable aging characteristics," in *Proc. 13th Conf. on Solid State Devices*, Tokyo, Japan, 1981; also *Japan. J. Appl. Phys.*, vol. 21, suppl. 21-1, pp. 435–436, 1982.

[16] K. Fujiwara, T. Fujiwara, K. Hori, and M. Takusagawa, "Aging characteristics of $Ga_{1-x}Al_xAs$ double-heterostructure lasers with

gold eutectic alloy solder," *Appl. Phys. Lett.*, vol. 34, pp. 668–670, May 1979.
[17] P. A. Kirkby and G.H.B. Thompson, "Channeled substrate buried heterostructure GaAs-(GaAl)As injection lasers," *J. Appl. Phys.*, vol. 47, pp. 4578–4589, Oct. 1976.
[18] E. Oomura, T. Murotani, H. Higuchi, H. Namizaki, and W. Susaki, "Low threshold current InGaAsP/InP buried crescent laser with double current confinement structure," *IEEE J. Quantum Electron.*, vol. QE-17, pp. 646–650, May 1981.
[19] R. E. Nahory and M. A. Pollack, "Threshold dependence on active-layer thickness in InGaAsP/InP DH lasers," *Electron. Lett.*, pp. 727–729, Nov. 1978.
[20] M. Ettenberg, C. J. Nuese, and H. Kressel, "The temperature dependence of threshold current for double-heterojunction lasers," *J. Appl. Phys.*, vol. 50, pp. 2949–2950, Apr. 1979.
[21] M. Yano, H. Imai, and M. Takusagawa, "Analysis of electrical, threshold, and temperature characteristics of InGaAsP/InP double-heterostructure lasers," *IEEE J. Quantum Electron.*, vol. QE-17, pp. 1954–1963, Sept. 1981.
[22] S. Yamakoshi, T. Sanada, O. Wada, I. Umebu, and T. Sakurai, "Direct observation of electron leakage in InGaAsP/InP double heterostructure," *Appl. Phys. Lett.*, vol. 40, pp. 144–146, Jan. 1982.
[23] H. Ishikawa, M. Yano, and M. Takusagawa, "Mechanism of asymmetric longitudinal mode competition in InGaAsP/InP lasers," *Appl. Phys. Lett.*, Apr. 1982.
[24] J. Shah, R. F. Leheny, and R. E. Nahory, and H. Temkin, "Hot-carrier effects in 1.3 m $In_{1-x}Ga_xAs_yP_{1-y}$ light emitting diodes," *Appl. Phys. Lett.*, vol. 39, pp. 618–620, Oct. 1981.
[25] K. Shima, K. Hanamitsu, T. Fujiwara, and M. Takusagawa, "Buried convex waveguide structure (GaAl)As injection lasers," *Appl. Phys. Lett.*, vol. 38, pp. 605–607, Apr. 1981.
[26] H. Ishikawa, H. Imai, T. Tanahashi, and M. Takusagawa, "Longitudinal mode behavior of transverse mode stabilized InGaAsP/InP double-heterostructure laser," *Appl. Phys. Lett.*, vol. 38, pp. 962–964, June 1981.
[27] M. Yamada, K. Mito, and T. Minakami, presented at the Nat. Conf. on Semiconductor Tech., IECE Japan, 1981, paper S5-1, unpublished.
[28] M. J. Adams, "Rate equations and transient phenomena in semiconductor lasers," *Opt- Electron.*, vol. 50, pp. 201–215, 1973.
[29] H. Imai, M. Morimoto, H. Ishikawa, K. Hori, M. Takusagawa, W. Wakita, M. Fukuda, and G. Iwane, "Accelerated aging test of InGaAsP/InP double-heterostructure laser diode with single transverse mode," *Appl. Phys. Lett.*, vol. 38, pp. 16–17, Jan. 1981.

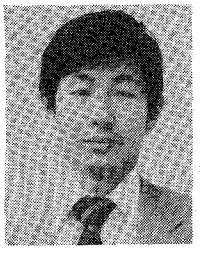

Hiroshi Ishikawa was born in Kokura, Japan, on November 22, 1946. He received the B.E. and M.E. degrees in electrical engineering from the Tokyo Institute of Technology, Tokyo, Japan, in 1970 and 1972, respectively.

He joined Fujitsu Laboratories, Ltd., Kawasaki, Japan, in 1972. He has been engaged in the research and development of GaAlAs lasers. Since 1980, he has been working on the research and development of InGaAsP/InP DH lasers.

Mr. Ishikawa is a member of the Institute of Electronics and Communication Engineers of Japan and the Japan Society of Applied Physics.

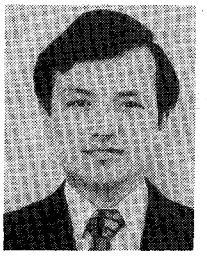

Hajime Imai (S'69–M'74) was born in Kagawa, Japan, on February 6, 1947. He received the B.E. degree in electrical engineering and the M.E. and Dr.Eng. degrees in electronics engineering from the University of Tokyo, Tokyo, Japan, in 1969, 1971, and 1974, respectively.

He joined the Fujitsu Laboratories, Ltd., Kawasaki, Japan, in 1974 and has been engaged in the research and development of semiconductor lasers.

Dr. Imai is a member of the Institute of Electronics and Communication Engineers of Japan and the Japan Society of Applied Physics.

Toshiyuki Tanahashi was born in Gifu, Japan, on September 4, 1953. He received the B.S. and M.S. degrees in physics from the University of Tokyo, Tokyo, Japan, in 1976 and 1978, respectively.

In 1978 he joined the Fujitsu Laboratories, Ltd., Kawasaki, Japan. Since then he has been engaged in the research of growth and characterization of III–V compound semiconductors for optical devices in the Semiconductor Materials Laboratory, Semiconductor Division, Fujitsu Laboratories, Ltd.

Mr. Tanahashi is a member of the Japan Society of Applied Physics.

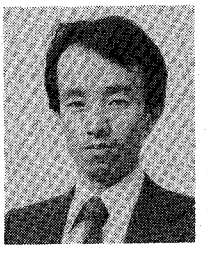

Ken-ichi Hori was born in Hyogo, Japan, on May 14, 1943. He received the B.E. degree in material science in 1966 from the University of Osaka, Osaka, Japan.

He joined the Research Department of Kobe Industries Corporation, Akashi, Japan, in 1966. Since 1973 he has been engaged in the study of semiconductor lasers at Fujitsu Laboratories, Ltd., Kawasaki, Japan.

Mr. Hori is a member of the Institute of Electronics and Communication Engineers of Japan and the Japan Society of Applied Physics.

Kenichiro Takahei was born in Ibaraki Prefecture, Japan, on July 31, 1946. He received the B.S. degree in physics from the Tokyo University of Education, Tokyo, Japan, in 1971, and the M.S. and Ph.D. degrees in physics from the University of Tokyo, Tokyo, Japan, in 1973 and 1976, respectively, while engaged in research on optical properties of thallous halides and their mixed crystals.

In 1976 he joined the Musashino Electrical Communication Laboratory, Nippon Telegraph and Telephone Public Corporation, Tokyo, Japan, where he has been engaged in research on the epitaxial growth of III–V compounds and development of semiconductor devices for optical fiber communications.

Dr. Takahei is a member of the Japan Society of Applied Physics.